PHYSICAL REVIEW B VOLUME 23, NUMBER 4 15 FEBRUARY 1981

Theory of the temperature dependence of the direct gap of germanium

P. B. Allen* and M. Cardona

Max-Planck-Institut für Festkörperforschung, Heisenbergstrasse 1, 7000 Stuttgart 80, Federal Republic of Germany

(Received 14 July 1980)

A complete pseudopotential calculation of the temperature dependence of the $\Gamma_{2'}$ conduction-band and the $\Gamma_{25'}$ valence-band states is performed. The calculation uses the lattice dynamics of Weber's bond-charge model and a local pseudopotential with a basis of 59 plane waves. Debye-Waller (DW) terms and also self-energy terms are included. While the DW terms alone are only slightly larger than experimental results, the addition of the self-energy correction results in a total shift of the gap with increasing temperature which is nearly three times as large as that observed. These results are compared with calculations and experiments for the second-order Raman scattering of c-Ge. We conclude that the pseudopotential–rigid-ion calculation overestimates the electron–2-TA-phonon coupling while it underestimates the coupling of the electrons with two TO phonons. The self-energy effects are particularly large for optical phonons connecting the $\Gamma_{25'}$ with the $L_{3'}$ valence bands.

I. INTRODUCTION

Semiconductors exhibit large shifts of the fundamental absorption edge with temperature,[1] either to the red (germanium-zinc blende[1]) or the blue [PbS, PbSe, PbTe (Ref. 2)]. Part of these shifts are due to thermal expansion and the concomitant changes in the band structure with volume. This effect, however, usually only accounts for a fraction ($\frac{1}{4}$ to $\frac{1}{2}$) of the observed shift. The remaining temperature effect is to be attributed to an *explicit* electron-phonon interaction,

$$\left(\frac{\partial E_g}{\partial T}\right)_P = \left(\frac{\partial E_g}{\partial T}\right)_V + \left(\frac{\partial E_g}{\partial \ln V}\right)_T \left(\frac{\partial \ln V}{\partial T}\right)_P$$

$$= \left(\frac{\partial E_g}{\partial T}\right)_V + \left(\frac{\partial E_g}{\partial \ln V}\right)_P \alpha\,, \qquad (1)$$

where α is the volume thermal-expansion coefficient. The first term in the right-hand side of Eq. (1) represents the "explicit" effect of the electron-phonon interaction while the second term contains the "implicit" term of the thermal expansion. The latter can be obtained either experimentally (from the pressure dependence of E_g) or theoretically (by calculating the band structure as a function of lattice constant). In either case it does not pose any serious conceptual problems.

The theory of the explicit effect of the electron-phonon interaction has attracted the attention of several workers since 1951, when Fan[3] presented a calculation of the electron self-energy due to phonons [first-order electron-phonon interaction $H_{\mathrm{ep}}^{(1)}$ in second-order perturbation theory, Fig. 1(a)] within a simple model (Debye phonons, parabolic bands). This model yields a decrease of the lowest gap with increasing T, in agreement with experiments for Ge-type materials but not for PbS. In 1955, Antončik[4] suggested calculating the temperature dependence of the band structure by using pseudopotential form factors weakened by a Debye-Waller (DW) term. The feeling was expressed that this theory and the Fan theory were in some sense equivalent, a feeling which to the present date has permeated a great deal of the literature on the subject. In a widely divulged but unpublished report, Brooks and Yu[5] showed that the DW terms stem from the second-order electron-phonon interaction to all orders while the Fan terms are the first-order interaction taken in second-order perturbation theory. They concluded, however, that the Fan terms are much smaller than the DW ones, and thus can be neglected, a conclusion which has more recently been realized to be erroneous.[6-10] Nevertheless, reasonable agree-

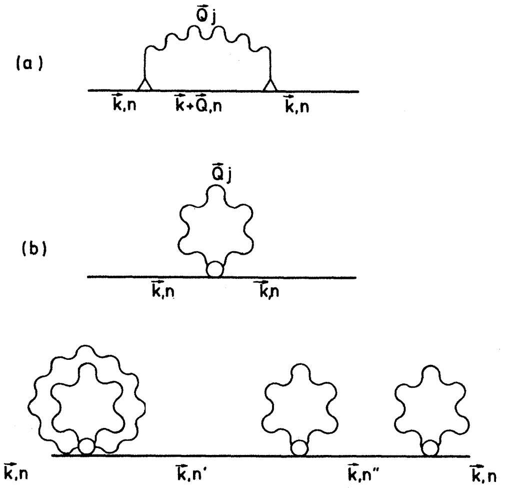

FIG. 1. Self-energy graphs corresponding to Eq. (2). Graph (a) is the Fan theory and corresponds to the second term of Eq. (2). Graph (b) is the lowest-order Debye-Waller correction and corresponds to the first term of Eq. (2). Graph (c) shows some higher-order Debye-Waller terms.

ment with experiment has been obtained in many cases by evaluating only the DW terms.[2,11,12]

In this paper we perform a complete pseudopotential calculation of the DW and self-energy contributions to the temperature dependence of the $\Gamma_{25'}$ valence and the $\Gamma_{2'}$ conduction bands of germanium. Our main assumption is a local pseudopotential, 59 plane waves, and the rigid-ion model. We evaluate explicitly the contribution of each phonon and each intermediate state to the self-energy. The DW contribution for a given band state is independent of the pair of phonons under consideration. The results obtained are listed separately for high-symmetry intermediate states in order to illustrate the origin of the dominant contributions.

The total temperature dependence of the E_0 gap $(\Gamma_{2'}-\Gamma_{25'})$ of germanium so calculated is two to three times higher than the experimental one, the relative discrepancy being larger at low temperatures. The DW term alone agrees better with the experiment although it is also larger. These results indicate that the theory overestimates the total electron–two-phonon interaction for TA phonons while underestimating it for TO phonons.

II. GENERAL FORMULAS

Consider a crystal with atoms of species κ which occupy sites $\vec{R}(\vec{l}\kappa)$ and have displacements $\vec{u}(\vec{l}\kappa)$ from the equilibrium, where $\vec{l}$ labels the unit cells. To second order in $\vec{u}$, the change in energy of an electronic state κn of unperturbed energy $\epsilon_{\vec{k}n}$ is

$$\Delta E_{\vec{k}n}=\sum_{\vec{l}\kappa,\vec{l}'\kappa'}\left\{\tfrac{1}{2}\langle\vec{k}n|\partial^2V/\partial R_\alpha(\vec{l}\kappa)\partial R_\beta(\vec{l}'\kappa')|\vec{k}n\rangle+\sum_{\vec{k}'n'}\frac{\langle\vec{k}n|\partial V/\partial R_\alpha(\vec{l}\kappa)|\vec{k}'n'\rangle\langle\vec{k}'n'|\partial V/\partial R_\beta(\vec{l}'\kappa')|\vec{k}n\rangle}{\epsilon_{\vec{k}n}-\epsilon_{\vec{k}'n'}}\right\}u_\alpha(\vec{l}\kappa)u_\beta(\vec{l}'\kappa'),\tag{2}$$

where $\partial V/\partial R_\alpha(\vec{l}\kappa)$ is the change in the self-consistent electron-lattice potential per unit displacement of the atom $\vec{l}\kappa$ in the α direction. The subscripts α, β, ... denote Cartesian components which are summed when repeated. The first term of (2) arises from the second-order electron-phonon interaction taken in first-order perturbation theory while the second is the first-order interaction in second-order perturbation theory. The displacements $\vec{u}$ are approximated as time independent. Later a thermal average will be taken over the ensemble of thermal displacements.

The condition of translational invariance[7] requires that if *every* atom is further displaced by a fixed amount, u_α, the energy does not change:

$$\Delta E_{\vec{k}n}(\{u_\alpha(\vec{l}\kappa)+u_\alpha\})=\Delta E_{kn}(\{u_\alpha(\vec{l}\kappa)\}).\tag{3}$$

This relation is valid for arbitrary small displacements $u_\alpha(\vec{l}'\kappa')$, in particular, take $u_\alpha(\vec{l}'\kappa')=u\,\delta_{\alpha\alpha'}\delta_{\vec{l}\vec{l}'}\delta_{\kappa\kappa'}$ (i.e., only one atom moves). Then Eqs. (2) and (3) impose the following relation between matrix elements of ∂V and ∂^2V:

$$0=\sum_{l'k'}\left\{\langle\vec{k}n|\partial^2V/\partial R_\alpha(\vec{l}\kappa)\partial R_\beta(\vec{l}'\kappa')|\vec{k}n\rangle+\sum_{\vec{k}'n'}\frac{\langle\vec{k}n|\partial V/\partial R_\alpha(\vec{l}\kappa)|\vec{k}'n'\rangle\langle\vec{k}'n'|\partial V/\partial R_\beta(\vec{l}'\kappa')|\vec{k}n\rangle}{\epsilon_{\vec{k}n}-\epsilon_{\vec{k}'n'}}+\sum_{\vec{k}'n'}\frac{\langle\vec{k}n|\partial V/\partial R_\beta(\vec{l}'\kappa')|\vec{k}'n'\rangle\langle\vec{k}'n'|\partial V/\partial R_\alpha(\vec{l}\kappa)|\vec{k}n\rangle}{\epsilon_{\vec{k}n}-\epsilon_{\vec{k}'n'}}\right\}.\tag{4}$$

This sum rule is valid for arbitrary $\alpha\beta,\vec{l}\kappa$, and guarantees that (2) vanishes as $\vec{Q}\rightarrow 0$ if $u_\alpha(\vec{l}\kappa)$ represents a long-wavelength acoustic phonon as was argued by Zeyher[13] and in Ref. 7. Thus (4) is a version of the "acoustic sum rule." Using (4), Eq. (2) can be rewritten in a form which explicitly exhibits translational invariance,

$$\Delta E_{\vec{k}n}=\sum_{\vec{l}\kappa,\vec{l}'\kappa'}\{\;\}[u_\alpha(\vec{l}\kappa)u_\beta(\vec{l}'\kappa')-\tfrac{1}{2}u_\alpha(\vec{l}\kappa)u_\beta(\vec{l}\kappa)-\tfrac{1}{2}u_\alpha(\vec{l}'\kappa')u_\beta(\vec{l}'\kappa')],\tag{5}$$

where the term $\{\;\}$ is the same in (2) and in (5).

The operators $\partial V/\partial R_\alpha$ and $\partial^2V/(\partial R_\alpha\partial R_\beta)$ must in principle be calculated self-consistently by working out the charge redistribution which accompanies an atomic displacement. In practice this calculation is frequently avoided, i.e., a guess or a "cookbook" prescription is used. Almost all such guesses are versions of the "rigid-ion approximation" which assumes that $\partial V/\partial R_\alpha$ and $\partial^2V/(\partial R_\alpha\partial R_\beta)$ are derivatives of an atomic potential. Ball[14] has shown that insofar as this is true, the atomic potentials sum to give the potential which determines the band structure,

$$V(\vec{r}) = \sum_{\vec{l}\kappa} V_\kappa(\vec{r} - \vec{R}(\vec{l}\kappa)). \tag{6}$$

If this model is used, it is clear that $-\partial^2 V/[\partial R_\alpha(l\kappa) \times \partial R_\beta(l'\kappa')]$ vanishes except for the term $\vec{l} = \vec{l}'$, $\kappa = \kappa'$. However, this term is omitted from the sum in Eq. (5) because the last factor vanishes.

Then Eq. (4) can be Fourier transformed and a thermal average performed, giving

$$\Delta E_{\vec{k}n}(T) \equiv \langle \Delta E_{\vec{k}n} \rangle = \sum_{\vec{Q}j} \partial E_{\vec{k}n}/\partial n_{\vec{Q}j}\,(n_{\vec{Q}j} + \tfrac{1}{2}), \tag{7}$$

where $n_{\vec{Q}j}$ is the Bose-Einstein occupation factor $(e^{\beta\omega_{\vec{Q}j}} - 1)^{-1}$ for the phonon mode $\vec{Q}j$ of energy $\omega_{\vec{Q}j}$. The coefficient $\partial E_{\vec{k}n}/\partial n_{\vec{Q}j}$ is

$$\begin{aligned}\partial E_{\vec{k}n}/\partial n_{\vec{Q}j} = \frac{1}{N}\sum_{\kappa\kappa'n'} \Bigg(& \frac{\langle \vec{k}n | \partial V/\partial R_\alpha(\kappa) | \vec{k}+\vec{Q}n' \rangle \langle \vec{k}+\vec{Q}n' | \partial V/\partial R_\beta(\kappa') | \vec{k}n \rangle}{\epsilon_{\vec{k}n} - \epsilon_{\vec{k}+\vec{Q}n'}} \\ & - \frac{\langle \vec{k}n | \partial V/\partial R_\alpha(\kappa) | \vec{k}n' \rangle \langle \vec{k}n' | \partial V/\partial R_\beta(\kappa') | \vec{k}n \rangle}{\epsilon_{\vec{k}n} - \epsilon_{\vec{k}n'}} \Bigg) e^{-i\vec{Q}\cdot(\vec{\tau}_\kappa - \vec{\tau}_{\kappa'})} \\ & \times \hbar\,(M_\kappa M_{\kappa'} \omega_{\vec{Q}j}^2)^{-1/2} \epsilon_\alpha(-\vec{Q}j, \kappa) \epsilon_\beta(\vec{Q}j, \kappa').\end{aligned} \tag{8}$$

In deriving this result, several conventions have been introduced. The lattice displacement is represented as

$$u_\alpha(\vec{l}\kappa) = \sum_{\vec{Q}j} (\hbar/2M_\kappa N\omega_{\vec{Q}j})^{1/2} \epsilon_\alpha(\vec{Q}j, \kappa) e^{i\vec{Q}\cdot(\vec{l}+\vec{\tau}_\kappa)} \phi_{\vec{Q}j}, \tag{9}$$

where M_κ is the mass of the κth atom located in the unit cell at position $\vec{\tau}_\kappa$, N is the number of unit cells in the crystal, and $\phi_{\vec{Q}j}$ is written in raising and lowering operators as $\phi_{\vec{Q}j} = a^\dagger_{\vec{Q}j} + a_{-\vec{Q}j}$. The polarization vectors $\epsilon_\alpha(\vec{Q}j, \kappa)$ obey the orthonormality and completeness relations

$$\begin{aligned}&\sum_\kappa \epsilon_\alpha(-\vec{Q}j, \kappa)\epsilon_\alpha(\vec{Q}j', \kappa) = \delta_{jj'}, \\ &\sum_j \epsilon_\alpha(-\vec{Q}j, \kappa)\epsilon_\beta(\vec{Q}j, \kappa') = \delta_{\alpha\beta}\delta_{\kappa\kappa'}.\end{aligned} \tag{10}$$

Bloch's theorem has been invoked in the form

$$\begin{aligned}&\sum_{\vec{l}} \langle \vec{k}'n' | e^{i\vec{Q}\cdot\vec{l}} \partial V/\partial R_\alpha(\vec{l}\kappa) | \vec{k}n \rangle \\ &\qquad = N\delta_{\vec{k}',\vec{k}+\vec{Q}} \langle \vec{k}+\vec{Q}, n' | \partial V/\partial R_\alpha(\kappa) | \vec{k}n \rangle,\end{aligned} \tag{11}$$

where $R_\alpha(\kappa)$ means $R_\alpha(\vec{l}\kappa)$ for the cell at the origin $\vec{l} = 0$. The factor of N in (11) comes from the $\vec{l}$ summation. We prefer to absorb this factor N into the wave functions so that in Eq. (8), electronic wave functions are normalized to 1 in a unit cell instead of in the whole crystal.

The perturbative formulas (7) and (8) can be directly related to the more conventional equations from diagrammatic perturbation theory.[8] The relevant diagrams are shown in Fig. 1. The first is the "usual" self-energy diagram, first evaluated by Fan.[3] The corresponding self-energy $\Sigma_\alpha(\vec{k}n, \omega)$ differs from our theory in having $\epsilon_{\vec{k}n}$ replaced by $\omega \pm \omega_{\vec{Q}j} + i\eta$ in the energy denominator, and $n_{\vec{Q}j} + \frac{1}{2}$ replaced by a more complicated set of Fermi and Bose functions. These differences arise because the diagrammatic method correctly accounts for the time dependence of the phonon amplitude. However, in semiconductors (or in metals except at low temperatures and at the Fermi level) the phonon frequency can be ignored in the denominator, and the position of the real part of the pole of the Green's function is given accurately by the replacement $\omega + i\eta \to \epsilon_{\vec{k}n}$. If this is done, diagram (a) gives exactly the first term of Eq. (8). The diagram (b) is the first term in the Taylor expansion of the Debye-Waller series (which was first discussed by Antončik[4]). When this graph is evaluated, it gives exactly the second term of Eq. (8) with no approximations required. In the next section these two parts of Eq. (8) will be discussed separately and labeled as the "self-energy" (SE) and "Debye-Waller" (DW) parts.

III. DIAMOND STRUCTURE

The starting equation (2) is exact to second order in the phonon amplitudes, and the final result (7) uses only the rigid-ion approximation. Otherwise, Eq. (7) is valid for all cases and crystal structures. In this section, the general result is applied to the diamond structure and for the case where $V(\vec{r} - \vec{R}(\vec{l}\kappa))$ is given by a local pseudopotential. The origin is taken midway between the atoms so that their coordinates are $\tau = \vec{\tau}_1 = -\vec{\tau}_2 = (1,1,1)a/8$. Because of inversion symmetry and time-reversal invariance,[15] the polarization vectors satisfy

$$\vec{\epsilon}(Qj, 1) = \vec{\epsilon}(Qj, 2)^*. \tag{12}$$

It is convenient[15] to make a unitary transformation to real variables

$$\begin{aligned}&\vec{\epsilon}(Qj, +) = [\vec{\epsilon}(Qj, 1) + \vec{\epsilon}(Qj, 2)]/\sqrt{2}, \\ &\vec{\epsilon}(Qj, -) = [\vec{\epsilon}(Qj, 1) - \vec{\epsilon}(Qj, 2)]/\sqrt{2}i.\end{aligned} \tag{13}$$

The magnitudes of $\epsilon(\vec{Q}j, +)^2$ and $\epsilon(\vec{Q}j, -)^2$ give the fraction of the mode Qj which is "acoustic" and "optic," respectively.

The electronic wave functions are eigenvectors of the secular equation

$$0=\sum_{\vec{G}'}\{[(\vec{k}+\vec{G})^2-\epsilon_{\vec{k}n}]\delta_{\vec{G}\vec{G}'}+V(\vec{G}-\vec{G}')S(\vec{G}-\vec{G}')\}c_{\vec{k}n}(\vec{G}'),$$

$$\psi_{\vec{k}n}=\Omega_c^{-1/2}\sum_{\vec{G}}c_{\vec{k}n}(\vec{G})e^{i(\vec{k}+\vec{G})\cdot\vec{r}}, \tag{14}$$

$$\sum_{G}c_{\vec{k}n}(\vec{G})^2=1,$$

where Ω_c is the volume of the unit cell, $V(\vec{G}-\vec{G}')$ is the local pseudopotential form factor [or Fourier transform of the local pseudopotential $V(\vec{r})$ normalized to the atomic volume], and $S(\vec{G})$ is the structure factor $\cos(\vec{G}\cdot\vec{\tau})$. The coefficients $c_{\vec{k}n}(\vec{G})$ can be (and are) chosen to be real.

Using these conventions, the matrix elements appearing in Eq. (8) are easily worked out:

$$\langle\vec{k}+\vec{Q},n'|\partial V/\partial R_\beta(\kappa')|kn\rangle=-ie^{-\vec{Q}\cdot\vec{\tau}_\kappa}[\Gamma_\beta(\vec{k}nn'\vec{Q})+(-1)^\kappa i\theta_\beta(\vec{k}nn'\vec{Q})],$$

$$\Gamma_\beta(\vec{k}nn'\vec{Q})\equiv\sum_{\vec{G}\vec{G}'}c_{\vec{k}+\vec{Q},n'}(\vec{G}')c_{\vec{k}n}(\vec{G})(\vec{G}'-\vec{G}+\vec{Q})_\beta V(\vec{G}'-\vec{G}+\vec{Q})\cos[(\vec{G}'-\vec{G})\cdot\vec{\tau}]. \tag{15}$$

The vector $\vec{\theta}$ is identical to $\vec{\Gamma}$ except that the cosine is replaced by the sine of the same argument. Finally the coefficient of Eq. (8) can be written

$$\partial E_{\vec{k}n}/\partial n_{\vec{Q}j}=(\partial E_{\vec{k}n}/\partial n_{\vec{Q}j})_{\rm SE}+(\partial E_{\vec{k}n}/\partial n_{\vec{Q}j})_{\rm DW},$$

$$(\partial E_{\vec{k}n}/\partial n_{\vec{Q}j})_{\rm SE}=\frac{1}{2}\sum_{n'}\frac{[\vec{\Gamma}(\vec{k}nn'\vec{Q})\cdot\vec{u}(\vec{Q}j+)+\vec{\theta}(\vec{k}nn'\vec{Q})\cdot\vec{u}(\vec{Q}j-)]^2}{\epsilon_{\vec{k}n}-\epsilon_{\vec{k}+\vec{Q}n'}},$$

$$(\partial E_{\vec{k}n}/\partial n_{\vec{Q}j})_{\rm DW}=-\frac{1}{2}\sum_{n'}\frac{[\vec{\Gamma}(\vec{k}nn'0)\cdot\vec{u}(\vec{Q}j+)]^2+[\vec{\Gamma}(\vec{k}nn'0)\cdot\vec{u}(\vec{Q}j-)]^2}{\epsilon_{\vec{k}n}-\epsilon_{\vec{k}n'}},$$

$$\vec{u}(\vec{Q}j\pm)\equiv(\hbar/M\omega_{\vec{Q}j})^{1/2}\vec{\epsilon}(\vec{Q}j\pm). \tag{16}$$

These equations are now in a form convenient for numerical calculations. The coefficient $\partial E_{\vec{k}n}/\partial n_{\vec{Q}j}$ has been expressed as the sum of two parts, labeled SE and DW.

IV. NUMERICAL PROCEDURE

Our aim is to evaluate the T-dependent energy shift [Eq. (7)] for the electron states at the fundamental gap (E_0gap) at $\vec{k}=0$ in Ge, i.e., for the Γ_2' conduction band and the $\Gamma_{25'}$ valence band. The choice of $\vec{k}=0$ simplifies the task because the coefficient $\partial E_{0n}/\partial n_{\vec{Q}j}$ then has full cubic symmetry; the sum over the Brillouin zone in (7) can be restricted to $\frac{1}{48}$th. We rewrite Eq. (7) as

$$\Delta E_{kn}(T)=\int_0^\infty d\Omega\, g^2F(\vec{k}n,\Omega)[(e^{\beta\Omega}-1)^{-1}+\tfrac{1}{2}], \tag{17}$$

$$g^2F(\vec{k}n,\Omega)\equiv\sum_{Qj}(\partial E_{\vec{k}n}/\partial n_{\vec{Q}j})\,\delta(\Omega-\omega_{\vec{Q}j}), \tag{18}$$

where g^2F is an electron-phonon spectral function reminiscent of the function $\alpha^2F(\Omega)$ in superconductivity. Both g^2F and α^2F are dimensionless (if Ω and $\epsilon_{\vec{k}n}$ are measured in the same units) densities of phonon states weighed by squared electron-phonon matrix elements. The difference is that in superconductivity only intermediate states around the initial energy (i.e., the Fermi energy) are considered, whereas here *all* intermediate states are included, weighted by their energy denominators.

We find that 89 Q points in the irreducible $\frac{1}{48}$th of the Brillouin zone are sufficient to give g^2F to quite good accuracy by using the tetrahedron method[16] including linear interpolation of the weights $\partial E_{\vec{k}n}/\partial n_{\vec{Q}j}$ as well as the frequencies $\omega_{\vec{Q}j}$.

The difficult part is the calculation of the weights $\partial E_{\vec{k}n}/\partial n_{\vec{Q}j}$. We have used a "rigid-pseudoion" model, consisting of attaching to each atom a local pseudopotential $V(\vec{r})$, which moves rigidly with the atom. The matrix elements $\langle a|\partial V/\partial\vec{r}|b\rangle$ are calculated using pseudo-wave-functions derived from the same pseudopotential whose derivative appears in the middle. The wave functions and energies depend only on $V(\vec{G})$, the pseudopotential Fourier transform at reciprocal-lattice vectors. These values we take from Cohen and Bergstresser.[17] The matrix elements depend also on $V(\vec{Q}+\vec{G})$, which we "derive" from $V(\vec{G})$ by smooth interpolation as indicated in Fig. 2. Also shown for comparison is the Heine-Abarenkov-Animalu "model potential" on the Fermi surface from Harrison's book.[18] We have used Harrison's values as a general guide in drawing our own curve. In particular, we have used the same value at $Q=0$, $-(\frac{2}{3})\epsilon_F$, where ϵ_F is the corresponding "free-electron" Fermi energy, although this is not rigorous. All we can say with certainty is that the "rigorous" value, $\sum_G\epsilon^{-1}(Q,Q+G)V_{\rm bare}(Q+G)$, tends to a constant as $Q\rightarrow0$ because of charge neutrality and the acoustic sum rule.[19] The val-

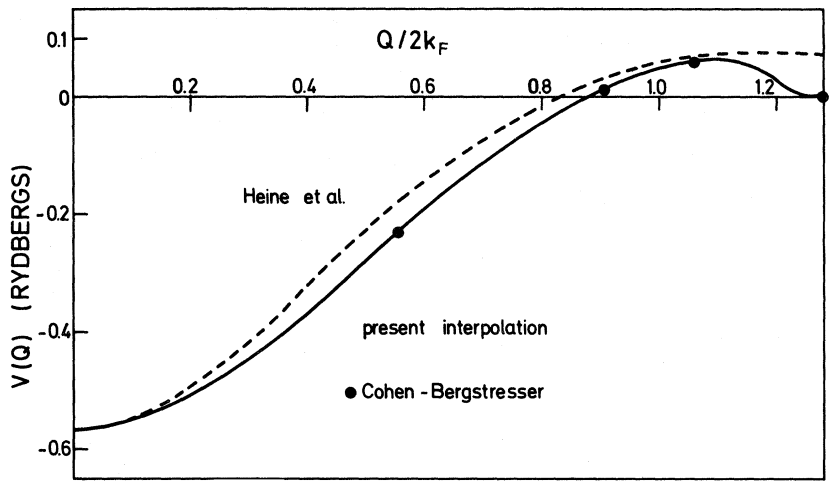

FIG. 2. The local pseudopotential $V(q)$ for Ge used in our calculations is interpolated through the empirical Cohen-Bergstresser values (Ref. 17) and follows roughly the Heine-Abarenkov-Animalu model potential (Ref. 18).

ue $-(\frac{2}{3})\epsilon_F$ is obtained using free-electron theory for ϵ^{-1} rather than band theory; use of the latter would exceed our computing capacity.

Having shamelessly abandoned rigor, it must be admitted that the aim of the present calculation is to make a reasonable model, satisfying all the sum rules, to study the sources of T dependence of $\epsilon_{\vec{k}n}$ in microscopic detail. However, in the final numerical answer a significant quantitative uncertainty must be assigned to the *ad hoc* nature of the model.

We have taken some care to ensure that the "rigid-pseudoion" model is the only significant source of uncertainty. The phonon frequencies and eigenvectors are derived from experiment *via* the excellent bond-charge-model parametrization of Weber.[20] The electronic energies and wave functions are derived by solving a 59×59 secular equation [Eq. (14)]. When a 15×15 secular equation is used,[21] the results are qualitatively similar but differ quantitatively by $\lesssim 20\%$. Three quantitative tests of the method were made, as described below.

(a) Translational invariance. In the derivation of Sec. II, the condition of translational invariance, Eq. (4), has been used to eliminate $\nabla^2 V$ in favor of ∇V in the final formulas. It is not necessary to do this. The matrix element of $\nabla^2 V$ is in fact easier to evaluate directly than by use of Eq. (4). The risk is that if either $\nabla^2 V$ or ∇V is inaccurate, then translational invariance will fail and $\partial E_{\vec{k}n}/\partial n_{\vec{Q}j}$ will not vanish as $Q \to 0$ for acoustic branches. Our programs use Eqs. (16), that is, $\nabla^2 V$ is *not* evaluated directly. However, we have verified that we obtain *exactly* (i.e., to better than four figures) the same answer by the direct evaluation. At first the exactness surprised us—we had anticipated a small error arising from the truncation at 59 plane waves. However, in retrospect it is clear that it is a unique property of plane waves to maintain translational invariance even in a truncated basis set. This is because plane waves are only changed by a phase when they are translated. Thus plane waves give equally good wave functions for a crystal before and after a translation, whereas tight-binding functions (for example) are tied to the original lattice sites and give a poor representation for the displaced lattice unless an infinite number of functions is used as a basis.[22] The fact that our calculation obeys the sum rule exactly is therefore only a good indication of no programming errors.

(b) Optic deformation potentials. The condition of translational invariance guarantees that $\partial E_{\vec{k}n}/\partial n_{\vec{Q}j}$ vanishes as $Q \to 0$ for j = an acoustic branch. When j is an optic branch, there is a separate test —we can calculate the shift directly by band theory with a "frozen-in" optic model deformation. The results are shown in Fig. 3. The nondegenerate $k = 0$ conduction band ($\Gamma_{2'}$) has only a shift to second order (as required by symmetry)

$$E(\Gamma_{2'},\vec{u}) = E(\Gamma_{2'},0) + D_{2'}u^2\,, \qquad (19)$$

whereas the degenerate $\Gamma_{25'}$ conduction-band state has its degeneracy lifted in first order. This is conveniently described by writing down the perturbation matrix for the $\Gamma_{25'}$ manifold. We choose basis functions $|1\rangle$, $|2\rangle$, and $|3\rangle$, which transform as yz, zx, and xy, respectively. Then group theory yields the following form to second order in the phonon displacement $\vec{u}$:

$$H_{\text{opt}} = \begin{bmatrix} D_a u^2 + D_b(3u_x^2 - u^2) & d_{25'}u_z + D_c u_x u_y & d_{25'}u_y + D_c u_x u_z \\ d_{25'}u_z + D_c u_x u_y & D_a u^2 + D_b(3u_y^2 - u^2) & d_{25'}u_x + D_c u_y u_z \\ d_{25'}u_y + D_c u_x u_z & d_{25'}u_x + D_c u_y u_z & D_a u^2 + D_b(3u_z^2 - u^2) \end{bmatrix} . \tag{20}$$

We made calculations for a distortion $\vec{u}_1 = -\vec{u}_2 = (0, 0, u)$. Following Eq. (19), this splits the $\Gamma_{25'}$ levels according to

$$E(\Gamma_{25'}, u) = \begin{cases} |d_{25'}u| + (D_a - D_b)u^2 , \\ (D_a + 2D_b)u^2 , \\ -|d_{25'}u| + (D_a - D_b)u^2 . \end{cases} \tag{21}$$

By analysis of Fig. 3, we find $D_{2'} = -2.7$ eV/Å^2, $d_{25'} = 11.7$ eV/Å, $D_a = 7.9$ eV/Å^2, and $D_b = 4.1$ eV/Å^2. The perturbative approach of Eq. (2) can also be used to calculate the second-order coefficients D, and we have been able to extract $D_{2'}$ and D_a directly from our computer codes for $E_{\vec{k}n}(T)$. The two methods agree to 1%, the accuracy being limited by the numerical differentiation of the nonperturbative results. This gives a second check on the internal consistency of our procedures.

It is possible to derive many of these results in a simple way. First we use the perturbative computer results to split D_a and $D_{2'}$ into Debye-Waller and self-energy components. These are

$$D_a^{\text{DW}} = 6.7 \text{ eV/Å}^2, \quad D_a^{\text{SE}} = 1.3 \text{ eV/Å}^2 ,$$

$$D_{2'}^{\text{DW}} = -0.75 \text{ eV/Å}^2, \quad D_{2'}^{\text{SE}} = -1.95 \text{ eV/Å}^2 .$$

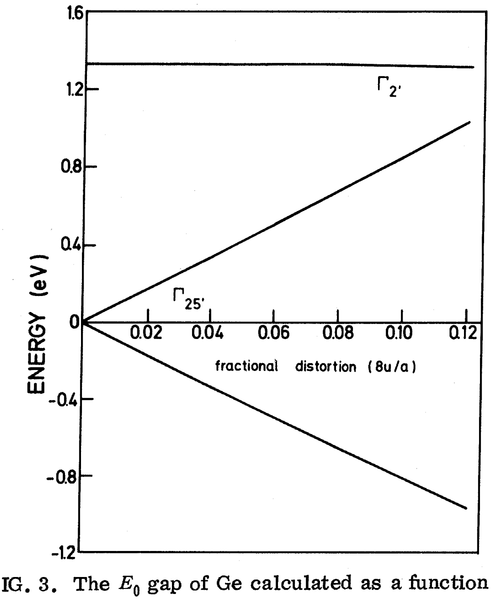

FIG. 3. The E_0 gap of Ge calculated as a function of optic-mode distortion amplitude. The atoms have been displaced by $\vec{u}_1 = -\vec{u}_2 = (0, 0, u)$. From these curves, first- and second-order deformation potentials are derived.

We point out again that the D^{DW} so obtained are independent of the pair of phonons under consideration. The coefficient D_b contains only self-energy contributions. Using the method of Ref. 23 it is possible to write analytic expressions for the coefficients of Eq. (20). For $d_{25'}$ and D_a^{DW} we find in a 15-plane-wave model

$$\begin{aligned} d_{25'} &= -\frac{4\pi}{a_0}[\beta^2(V_4 - V_{12}) + \gamma\beta\sqrt{2}(V_3 - V_{11})] , \\ D_a^{\text{DW}} &= \left(\frac{2\pi}{a_0}\right)^2 [4\beta^2 V_8 + \beta\gamma\sqrt{2}(-3V_3 + 11V_{11})] , \end{aligned} \tag{22}$$

where $\beta = 0.83$ and $\gamma = 0.55$. Equations (22) with the pseudopotential form factors of Fig. 2 yield $d_{25'} = 10.5$ eV/Å and $D_a^{\text{DW}} = 5.2$ eV/Å^2, in reasonable agreement with the numbers given above. The deformation potentials d_0 and D_1 are usually found in the literature[23,24] instead of the ones given above. They are defined as[23-25]

$$\begin{aligned} d_0 &= (a_0/\sqrt{3})d_{25'} \simeq 38 \text{ eV} , \\ D_1(\Gamma_{25'}) &= \tfrac{3}{4}D_a a_0^2 = 200 \text{ eV} , \\ D_1(\Gamma_{2'}) &= \tfrac{3}{4}D_{2'} a_0^2 = -65 \text{ eV} . \end{aligned} \tag{23}$$

The coefficient $d_{25'}$ governs the strength of resonant first-order Raman scattering, as will be described in a subsequent paper. Its magnitude agrees reasonably with others found in the literature for Ge and other zinc-blende-type materials.[23-25] Pötz and Vogl[26] have also performed this type of analysis for Ge and a variety of other semiconductors using a tight-binding approach. They found approximate consistency between tight-binding and pseudopotential methods. Their pseudopotential value of d_0 agrees well with ours. Also they have pointed out that the spin-orbit interaction, ignored in our work, has a drastic effect on the $Q = 0$ optic-mode coupling, namely, that the linear splitting of Eq. (20) is reduced by a factor $\sqrt{3}$ (because one of the states is split off by 0.3 eV) but the quadratic shifts are greatly enhanced (by amounts of order $|d_{25'}|^2/\Delta \sim 500$ eV/Å^2), because the off-diagonal linear terms $d_{25'}u_i$ cause the spin-orbit split bands to mix and repel in energy.[23] At first it might seem that our results ignoring the spin-orbit interaction would therefore be meaningless. However, for wave vectors Q larger than about $\frac{1}{10}$th of the Brillouin-zone boundary, the energy denominators $\epsilon_{\vec{k}n} - \epsilon_{\vec{k}+\vec{Q}n'}$ will be sufficiently larger than Δ so that the spin-orbit effect can be safely ignored.

(c) Debye-Waller effect. There is another sensitive check of our numerical procedure, namely, by direct calculation of the Debye-Waller effect. In other words, in the secular equation (14) the pseudopotential form factor $V(\vec{G})$ can be replaced by

$$V(\vec{G})\exp(-G^2\langle u^2\rangle/2)\,, \qquad (24)$$

where $\langle u^2\rangle$ is the mean-square thermal vibrational amplitude. Equation (24) includes not only the second-order terms of Fig. 1(b) but also all higher-order terms of the form shown in Fig. 1(c). The resulting eigenvalues $E_{kn}(T)$ should be compared with the results from Eqs. (7) and (17) using only the second-order Debye-Waller part of $\partial E_{\vec{k}n}/\partial n_{Qj}$ from Eq. (16) in Eq. (17). This comparison is made in Fig. 4. At low temperatures the different procedures agree to about 1%, whereas by 500 K there are discrepancies of 18% in the conduction band and 4% in the valence band. These discrepancies reflect the influence of corrections of higher order in u/a [Fig. 1(c)]. These results demonstrate both the correctness of the perturbative treatment and the low "noise" level in the calculation arising from finite mesh size and similar sources. As a further check we have added to Fig. 4 our calculated average vibrational amplitudes compared with x-ray determinations.[27]

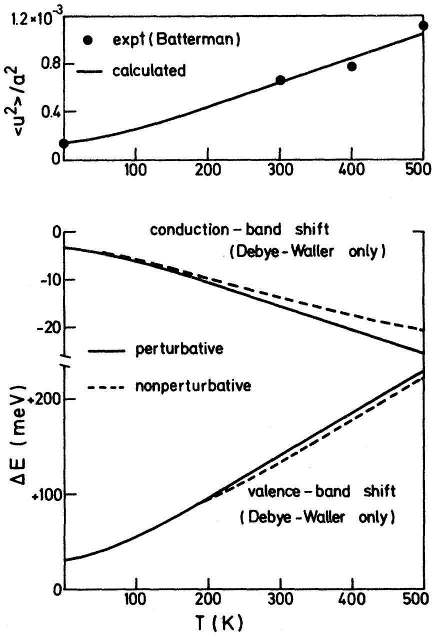

FIG. 4. Temperature dependence of mean-square displacement $\langle u^2\rangle$ normalized to the lattice constant a (solid line) as compared with experimental x-ray data [B. W. Batterman and D. R. Chipman, Phys. Rev. 127, 690 (1962)]. Also, temperature dependence of the Debye-Waller part of the temperature shift of the $\vec{k}=0$ valence ($\Gamma_{25'}$) and conduction ($\Gamma_{2'}$) bands. The solid curve is the calculation by perturbation theory to order $(u/a)^2$ using Eqs. (16), and the dashed curve is obtained by solving exactly the secular equation including Debye-Waller factors [pseudopotentials of Eq. (24)]. Notice that the energy scale for the valence band differs by a factor 5 from that for the conduction band. At 500 K, the gap has narrowed from 1.33 to 1.08 eV (including only Debye-Waller corrections).

There remains a significant numerical problem in summing the self-energy terms $(\partial E/\partial n_{\vec{Q}j})_{\mathrm{SE}}$ of Eq. (15) over the Brillouin zone to evaluate Eq. (17), especially since the energy denominators occasionally vanish. An advantage of confining our calculation to electronic states at $\vec{k}=0$ is that for the valence band there are no small denominators except the intraband terms, as Q goes to zero. Acoustic phonons create no problem here; the matrix elements in the numerator approach zero at the same rate. The $Q=0$ optic phonons have $\Gamma_{25'}$ symmetry which means there is no allowed matrix element in the conduction band at $k=0$ $(\Gamma_{2'})$ as $\vec{Q}$ goes to zero, but there is one for the valence band. Thus an integral of the type $\sum_{\vec{Q}} Q^{-2}\delta(\omega-\omega_{\mathrm{opt}})$ is encountered for the valence band. The Q^{-2} divergence cancels against the Q^2dQ phase-space factor, which means that with a fine enough mesh the integral will converge. Our 89-point mesh is coarse in this respect, and therefore special care is needed. The problem is more severe in the conduction band because the $\vec{k}=0$ $(\Gamma_{2'})$ state is degenerate with a constant energy surface near the Brillouin-zone boundary. In this case the integral is of the type $\int dQ(Q-Q_0)^{-1}$ and gives a finite answer when the principal part is correctly taken. However, numerical integration schemes using meshes not specially adapted to this surface will not converge properly, no matter how fine the mesh. Fortunately, we found that the results for $E_{n\vec{k}}(T)$ did not depend sensitively on this part of phase space, provided elementary precautions were taken. We tried two different procedures. First, the 89 mesh points were examined and two were discovered which had particularly small energy denominators for conduction-band states, namely, $\vec{k}=(0.625,0,0)$ with $\Delta\epsilon=+0.0006$ Ry, and $\vec{k}=(0.875,0.875,0)$ with $\Delta\epsilon=-0.0028$ Ry. In each case, only one phonon coupled in a $\Gamma_{2'}\rightarrow\vec{k}$ transition, and the anomalously large value of $\partial\epsilon_{\vec{k}=0,n}/\partial n_{\vec{Q}j}$ was artificially set to zero. All other denominators exceeded 0.006 Ry in magnitude. The second procedure was a Lorentzian broadening of each denominator by $\Delta=0.01$ Ry. In other words, $(\Delta\epsilon)^{-1}=(\epsilon_{kn}-\epsilon_{k'n'})^{-1}$ was replaced by $\Delta\epsilon/[(\Delta\epsilon)^2+\Delta^2]$. This corresponds to giving each electron a complex self-energy with $\mathrm{Im}\Sigma=1/2\tau=0.005$ Ry. If the Rayleigh-Schrödinger perturbation theory used here were replaced by

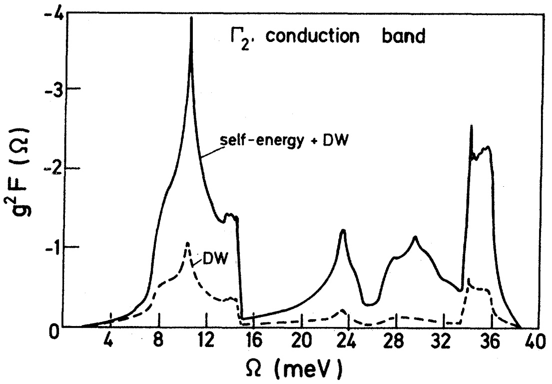

FIG. 5. Spectral dependence of the function g^2F for the $\Gamma_{2'}$ lowest conduction band of germanium. Debye-Waller (dashed) and total (DW+ SE) solid-line effects.

the more realistic Feynman perturbation theory, each state would be automatically endowed with a complex self-energy, but the magnitude of $\mathrm{Im}\Sigma$ could vary considerably with $\vec{k}n$. The value 0.005 Ry would be fairly normal for states at the Fermi surface of a metal under electron-phonon scattering. It is hard to estimate a realistic value for Ge, but 0.005 Ry is probably an overestimate. The reason for choosing such a large value was that a smaller one would not have been effective in smoothing the noise arising from the finite-mesh size of our calculation. The final result for $\epsilon_{n\vec{k}}(T)$ was not sensitive to the prescription used to handle the integration difficulties.

V. RESULTS AND DISCUSSION

We have evaluated numerically the function $g^2F(\vec{k}n,\Omega)$ for $\vec{k}=0$ and n either the $\Gamma_{2'}$ or the $\Gamma_{25'}$ gap states. This function consists, as already mentioned, of a DW and an SE contribution. The DW contributions and the total g^2F are shown in Figs. 5–7 for $\Gamma_{2'}$, $\Gamma_{25'}$ and the E_0 gap ($\Gamma_{2'}-\Gamma_{25'}$), respectively. These figures clearly show the cancellation of DW and SE contributions as $\Omega\rightarrow 0$. By replacing the results of Fig. 7 into Eq. (17), we obtain the temperature dependence of E_0 shown in Fig. 8 (both DW term and total = DW+ SE). We have also plotted in Fig. 8 the experimental data[1,27] and the result of subtracting from these data the thermal expansion effect of Eq. (1), using the expansion coefficient of Ref. 28 and the deformation potential ($\partial E_g/\partial \ln V$) of Ref. 29. The calculated total explicit electron-phonon-interaction effect (DW+ SE) is three times larger than the observed one (experiment minus thermal expansion). The relative discrepancy, however, decreases with increasing temperature. We encounter the paradoxical result that the DW term alone accounts better for the experimental results than the com-

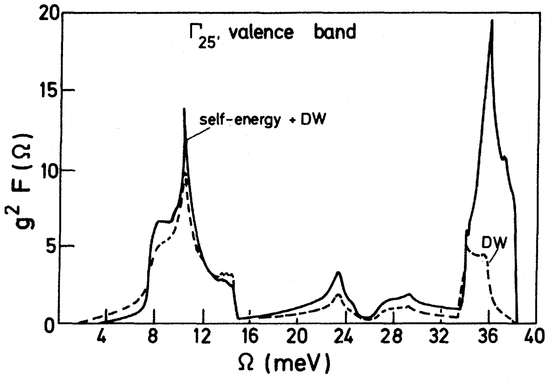

FIG. 6. Spectral dependence of the function g^2F for the $\Gamma_{25'}$ valence band of germanium. DW and total (DW+ SE) effects.

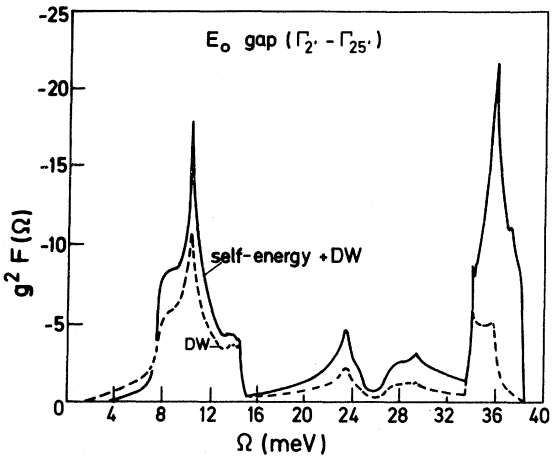

FIG. 7. Spectral dependence of the function g^2F for the E_0 gap of germanium obtained by subtracting the curves of Fig. 7 from those of Fig. 6.

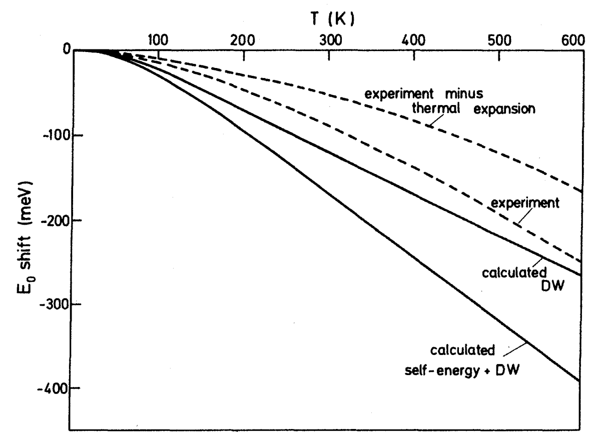

FIG. 8. Temperature dependence of the E_0 gap of germanium. Solid lines calculated DW or total (DW+ SE) contributions. Dashed lines: experimental shift (Ref. 1) and this shift minus effect of thermal expansion.

plete DW+SE. This, of course, is the reason for the large number of calculations in the literature considering only DW terms[2,11,12]: they are much easier and agree better with experiments than the complete job. The spectral distribution of $g^2F(\Omega)$ has two main sharp peaks associated with the TA (centered at 11 meV) and the TO (centered at 36 meV) phonons at the edge of the zone, respectively. They account for the recent success of Manoogian and Leclerc[30] in fitting the observed temperature dependence of E_0 in Ge to two oscillators at 15 and 34 meV, respectively.

The decrease in the discrepancy between theory and experiment with increasing temperature suggests that the present calculation overestimates the electron–2TA-phonon interaction while underestimating that with 2TO phonons. A calculation of the second-order Raman spectrum by the same method used here[31] leads to the same conclusion. It seems inescapable that the fault lies in our rigid-pseudopotential model. The correct procedure requires replacing the gradient of the pseudopotential in Eq. (2) by a more complicated quantity

$$\frac{\partial V(\vec{r})}{\partial R_\alpha(\vec{l}\kappa)} \rightarrow \int d\vec{r}'\epsilon^{-1}(\vec{r},\vec{r}')\frac{\partial V_b(\vec{r}')}{\partial R_\alpha(\vec{l}\kappa)}\ , \tag{25}$$

where V_b is the bare pseudopotential and ϵ^{-1} is a dielectric function which gives a proper account of the charge redistribution when an atom moves. If the pseudopotential were so weak that V equaled $\epsilon^{-1}V_b$ *and* if $\epsilon^{-1}(r,r')$ depended only on $\vec{r}-\vec{r}'$, then the model used here would be exact. Short of doing a complete calculation of ϵ^{-1}, it is hard to estimate the accuracy of our model. However, as Ball[14] has argued, there can always be a component of (25) which is transverse (i.e., not equal to the gradient of any scalar field) and thus fundamentally nonrigid. A reasonable hypothesis to explain qualitatively our discrepancy with experiment is the following: Assume there is a significant nonrigid charge redistribution out of bonds which are stretched and into bonds which are compressed. This ought to enhance the scattering from optical phonons where significant stretching and compression of bonds occurs. If simultaneously there is a net weakening of the rigid part of the potential, this should have the desired effect of weakening the TA coupling and enhancing the TO coupling.

TABLE I. Electron–two-phonon deformation potentials D_1 (in eV) for the $\Gamma_{2'}$ conduction-band states and two phonons at the X point. The table includes the separate contributions of the eight lowest X intermediate states to the self-energy.

		X-point phonons		
Intermediate state		TA	LA and LO	TO
Valence bands	X_1	0	0	0
	X_4	0	0	0
Conduction bands	X_1	0	1810	0
	X_4	–3	0	–25
	DW	–18	–18	–18
Total	$D_1(\Gamma_{2'})$	–74	1780	–50

TABLE II. Electron–two-phonon deformation potentials D_1 (in eV) for the $\Gamma_{25'}$ valence states and two phonons at the X point. The table includes the separate contributions of the eight lowest X intermediate states to the self-energy.

		X-point phonons		
Intermediate state		TA	LA and LO	TO
Valence bands	X_1	100	43	12
	X_4	167	255	0
Conduction bands	X_1	–3	–120	–165
	X_4	–71	–30	0
	DW	161	161	161
Total	$D_1(\Gamma_{25'})$	355	250	–20

In Sec. IV we gave the deformation potential $D_1(\Gamma_{25'})$ [Eq. (23)] which represents the interaction of two optical phonons with the $\Gamma_{25'}$ and the $\Gamma_{2'}$ states. In Tables I–IV we present the corresponding deformation potentials for the two phonons at X (Tables I and II), at L (Tables III and IV), and at W (Table V). The tables list the total D_1, the Debye-Waller contribution, and the separate contributions to the SE using as intermediate states the four lowest-energy bands. The main contribution to the SE arises for the LA and LO phonons with the X_1 conduction-band state as intermediate state and for the TA and TO phonons with the $L_{3'}$ valence band as intermediate state. The reason for these large contributions is, at least in part, the small corresponding energy denominators

TABLE III. Electron–two-phonon deformation potentials D_1 (in eV) for the $\Gamma_{2'}$ conduction state and two phonons at the L point. The table includes the separate contributions of the eight lowest L intermediate states to the self-energy.

		L-point phonons			
Intermediate state		TA	LA	LO	TO
Valence bands	$L_{2'}$	0	0	0	0
	L_1	0	1	1	0
	$L_{3'}$	4	0	0	4.4
Conduction bands	L_1	0	344	341	0
	L_3	–16	0	0	–17
	$L_{2'}$	0	2	–2	0
	DW	–18	–18	–18	–18
Total	$D_1(\Gamma_{2'})$	–67	304	300	–65

TABLE IV. Electron–two-phonon deformation potentials D_1 (in eV) for the $\Gamma_{25'}$ conduction states and two phonons at the L point. The table includes the separate contributions of the eight lowest L intermediate states to the self-energy.

Intermediate state		L-point phonons TA	LA	LO	TO
Valence bands	$L_{2'}$	59	6.3	5	60
	L_1	0	88	89	0
	$L_{3'}$	645	195	199	642
Conduction bands	L_1	−27	−73	−72	−28
	L_3	−51	−11	−11	−51
	$L_{2'}$	0	0	0	0
	DW	161	161	161	161
Total	$D_1(\Gamma_{25'})$	723	267	272	721

TABLE V. Electron-phonon deformation potential D_1 (in eV) for the $\Gamma_{2'}$ conduction-band state and the $\Gamma_{25'}$ valence states and two phonons at the W point. The table also gives the Debye-Waller contribution to D_1.

		W-point phonons TA	LA and LO	TO
Debye-Waller	$\Gamma_{2'}$	−18	−18	−18
Total	$D_1(\Gamma_{2'})$	−65	−96	−61
Debye-Waller	$\Gamma_{25'}$	161	161	161
Total	$D_1(\Gamma_{25'})$	113	280	102

($\Gamma_{25'}-L_{3'}\simeq 1.07$ eV, $\Gamma_{2'}-X_1\simeq 0.08$ eV). The total contribution to g^2F of the LA and LO bands, however, is small (see Figs. 5 and 6). The large SE contribution to $D_1(\Gamma_{25'})$ for TA and TO phonons is the main contributor to the temperature dependence of E_0. The total $D_1(E_0)$ for TA and TO phonons is $\simeq$720 eV. No independent determination of these deformation potentials is available for Ge. For GaAs, however, $D_1(E_0)$ has been evaluated to be 2600 eV from the second-order Raman spectrum.[20] For Ge, D_1 has been determined from Raman measurements at the E_1 gap (2.1 eV). It amounts to 2500 eV for TO and 170 eV for TA phonons.[32] Under the assumption that the D_1 deformation potentials are about the same at E_1 as at E_0 we conclude that the calculations presented here (Tables I–IV) overestimate the $D_1(\Gamma_{25'})$ for TA and underestimate it for TO phonons. This conclusion corroborates the analysis given above.

Further details of the individual two-phonon deformation potentials will be given in a subsequent paper[33] on the alteration of phonon frequencies by doping. The calculated values of $\partial\epsilon_{\vec{k}n}/\partial n_{\vec{Q}j}$ will be plotted versus $\vec{Q}$ along symmetry lines. Experimental measurement of the effect of doping on TA and TO phonons would provide independent clarification of the analysis given here.

ACKNOWLEDGMENTS

We thank P. Vogl and R. Zeyher for useful discussions, and H.-J. Mattausch for tetrahedron programs. PBA thanks H. Bilz for hospitality at the MPI-FKF, Stuttgart, and acknowledges partial support by NSF, Grant No. DMR7900837.

---

*Permanent address: State University of New York, Stony Brook, N.Y. 11794.

[1] Y. P. Varshni, Physica (Utrecht) 34, 149 (1967); M. L. Cohen and D. J. Chadi, in *Semiconductor Handbook*, edited by M. Balkanski (North-Holland, Amsterdam, 1980), Vol. 2, Chap. 4b.

[2] C. Keffer, T. M. Hayes, and A. Bienenstock, Phys. Rev. Lett. 21, 1676 (1968).

[3] H. Y. Fan, Phys. Rev. 82, 900 (1951).

[4] E. Antončik, Czech. J. Phys. 5, 449 (1955).

[5] H. Brooks and S. C. Yu (unpublished).

[6] K. Baumann, Phys. Status Solidi B 63, K71 (1974).

[7] P. B. Allen and V. Heine, J. Phys. C 9, 2305 (1976).

[8] P. B. Allen, Phys. Rev. B 18, 5217 (1978).

[9] C. S. Guenzer and A. Bienenstock, Phys. Rev. B 8, 4655 (1973).

[10] M. Schlüter, G. Martinez, and M. L. Cohen, Phys. Rev. B 12, 650 (1975).

[11] P. Y. Yu and M. Cardona, Phys. Rev. B 3, 305 (1971).

[12] D. Auvergne, J. Camassel, H. Mathieu, and M. Cardona, Phys. Rev. B 9, 5168 (1974).

[13] R. Zeyher, in *Light Scattering in Solids*, edited by M. Balkanski, R. C. C. Leite, and S. P. S. Porto (Flammarion, Paris, 1976), p. 87.

[14] M. A. Ball, J. Phys. C 8, 3328 (1975).

[15] M. Lax, *Symmetry Principles in Solid State and Molecular Physics* (Wiley, New York, 1974).

[16] G. Lehmann and M. Taut, Phys. Status Solidi B 54, 469 (1972); 57, 815 (1973).

[17] M. L. Cohen and T. K. Bergstresser, Phys. Rev. 141, 789 (1966).

[18] W. A. Harrison, *Pseudopotentials in the Theory of Metals* (Benjamin, New York, 1966).

[19] P. Vogl, Phys. Rev. B 13, 694 (1976); also, in *Physics of Nonlinear Transport in Semiconductors*, edited by D. K. Ferry, J. R. Barker, and C. Jacobini (Plenum, New York, 1980).

[20] W. Weber, Phys. Rev. B 15, 4789 (1977); O. H. Nielsen and W. Weber, Comput. Phys. Commun. 18, 101 (1979).

[21] M. Cardona and F. H. Pollak, Phys. Rev. 142, 530 (1966).

[22] S. K. Sinha, Phys. Rev. 169, 477 (1968).

[23] M. Cardona, in *Atomic Structure and Properties of*

Solids, edited by E. Burstein (Academic, New York, 1972).

[24] R. Trommer and M. Cardona, Phys. Rev. B 17, 1865 (1978).

[25] J. D. Wiley, in *Semiconductors and Semimetals*, edited by R. K. Willardson and A. C. Beer (Academic, New York, 1975), Vol. 10, p. 133.

[26] V. Pötz and P. Vogl (unpublished).

[27] T. P. McLean, in *Progress in Semiconductors* (Heywood, London, 1960), Vol. 5, p. 53.

[28] D. F. Gibbons, Phys. Rev. 112, 136 (1958).

[29] B. Welber, M. Cardona, Y. F. Tsay, and B. Bendow, Phys. Rev. B 15, 875 (1977).

[30] A. Manoogian and A. Leclerc, Can. J. Phys. 57, 1766 (1979).

[31] P. B. Allen and M. Cardona (unpublished).

[32] J. B. Renucci, M. Renucci, R. Zeyher, and M. Cardona, Phys. Rev. B 16, 4309 (1974).

[33] P. B. Allen and M. Cardona (unpublished).